Original Articles

Drug library screen reveals benzimidazole derivatives as selective cytotoxic agents for KRAS-mutant lung cancer

Iwao Shimomura[a,b], Akira Yokoi[a], Isaku Kohama[a], Minami Kumazaki[a], Yuji Tada[b], Koichiro Tatsumi[b], Takahiro Ochiya[a], Yusuke Yamamoto[a,*]

[a] *Division of Molecular and Cellular Medicine, National Cancer Center Research Institute, 5-1-1 Tsukiji, Chuo-ku, Tokyo, 104-0045, Japan*
[b] *Department of Respirology, Graduate School of Medicine, Chiba University, 1-8-1 Inohana, Chuo-ku Chiba-shi, Chiba, 260-8670, Japan*

ARTICLE INFO

ABSTRACT

KRAS is one of the most frequently mutated oncogenes in human non-small cell lung cancer (NSCLC). Mutations in KRAS are detected in 30% of NSCLC cases, with most of them occurring in codons 12 and 13 and less commonly in others. Despite intense efforts to develop drugs targeting mutant KRAS, no effective therapeutic strategies have been successfully tested in clinical trials. Here, we investigated molecular targets for KRAS-activated lung cancer cells using a drug library. A total of 1271 small molecules were screened in KRAS-mutant and wild-type lung cancer cell lines. The screening identified the cytotoxic effects of benzimidazole derivatives on KRAS-mutant lung cancer cells. Treatments with two benzimidazole derivatives, methiazole and fenbendazole—both of which are structurally specific—yielded significant suppression of the RAS-related signaling pathways in KRAS-mutated cells. Moreover, combinatorial therapy with methiazole and trametinib, a MEK inhibitor, induced synergistic effects in KRAS-mutant lung cancer cells. Our study demonstrates that these benzimidazole derivatives play an important role in suppressing KRAS-mutant lung cancer cells, thus offering a novel combinatorial therapeutic approach against such cancer cells.

1. Introduction

Lung cancer is the leading cause of death worldwide, estimated to account for more than one million deaths per year [1]. Non-small cell lung cancer (NSCLC)—the main histological type comprising adenocarcinoma, squamous carcinoma, and large cell carcinoma—accounts for approximately 85% of all lung cancer cases [2]. Unfortunately, the prognosis of lung cancer remains dismal, with a five-year survival rate of approximately 15% [3]. Cytotoxic chemotherapy has improved the prognosis of both early- and advanced-stage NSCLC, and new advances in the discovery of oncogenic drivers as well as specific targeted therapies have yielded significant improvements in outcomes and quality of life of NSCLC patients [4].

In recent years, many studies have focused on mutations in epidermal growth factor receptor (EGFR) and anaplastic lymphoma kinase (ALK) in NSCLC patients [5,6]. Specific targeted agents, such as gefitinib and crizotinib, designed to treat NSCLC, are known to be effective in patients [7,8]. Mutations of the RAS family are detected in up to ∼30% of human cancers, with 20–30% of NSCLC patients carrying KRAS mutations [9–11]. The function and importance of KRAS as a GTPase are evidenced from its role in connecting upstream signals from cell surface receptors, such as those in the FGFR and ERBB families to the MAPK cascade and other cancer-associated pathways [12]. Although KRAS signaling is a major oncogenic driver of lung cancers and is associated with a poor prognosis and therapy resistance, effective targeted therapy for KRAS-mutated lung cancer patients is currently lacking [13]. While indirect strategies such as synthetic lethality have emerged [14], novel treatment strategies to combat this major oncogenic mutation are urgently needed.

Most studies in past decades have sought to develop drugs that target the downstream effectors of KRAS. Mutant-activated KRAS mediates several key functions, including those involving intracellular signaling pathways that regulate cell proliferation, differentiation, and survival [15,16]. Activation of KRAS leads to the stimulation of

signaling pathways, including the PI3K/AKT and RAF/MEK/ERK pathways [17]. Several studies have demonstrated that mutations in the kinases of these so-called 'canonical' RAS signaling pathways are frequently observed in human cancer, identifying them as suitable therapeutic targets [18,19]. With advances in molecular biology and high-throughput methodologies, as well as developments in genome sequencing, researchers now employ target-based screening for new drug discovery [20]. However, the target-based discovery of oncological drugs has been less successful than initially predicted. Reviews have shown that an alternative, phenotype-based approach with small molecule libraries has played a prominent role in the discovery of new chemical probes [21]. Consequently, there is a trend in drug discovery of cancer therapeutics toward phenotypic screening to provide greater confidence that the molecules discovered will deliver the desired therapeutic efficacy [22]. Small-molecule libraries that have a well-annotated pharmacology are suitable for phenotypic screening. Here, we used the Prestwick Chemical Library® (PCL)—a library comprising more than 1200 drugs approved by the FDA, EMA, and other agencies.

Based on our screening results using the chemical library, we identified the biological effects of benzimidazole derivatives, such as methiazole, fenbendazole, carbendazim, and benzimidazole itself on KRAS-mutant lung cancer cells. Moreover, we determined the molecular mechanism of these compounds. Our data provide novel insights for targeting KRAS-mutant lung cancer cells, thereby advancing the development of future therapeutics.

2. Materials and methods

2.1. Cell culture

All the human lung cancer cell lines were purchased from American Type Culture Collection (ATCC, Manassas, VA, USA). Detailed information about the cell lines and culturing methods is described in Table S1.

2.2. Drug treatment

The Prestwick Chemical Library® was purchased from Prestwick Chemical (Illkirch-Graffenstaden, France). This library contains 1271 small molecules, 95% of which are approved drugs (FDA, EMA, and other agencies). Methiazole was obtained from Latoxan (Portes-lès-Valence, France). Fenbendazole, benzimidazole, carbendazim, oxibendazole, mebendazole, albendazole, and fluticasone propionate were obtained from TCI Chemicals (Tokyo, Japan). Nocodazole was obtained from Wako (Tokyo, Japan). Estramustine was obtained from Sigma-Aldrich (St. Louis, MO, USA). Vemurafenib, dabrafenib, and trametinib were obtained from Selleck (Houston, TX, USA). The drugs were prepared at 10 µM by dissolving in DMSO for each analysis.

2.3. Cell proliferation assay

Cell proliferation was evaluated using the CellTiter-Glo® 2.0 Assay (Promega, Madison, WI, USA) as described in the manufacturer's instructions. Each cell line was seeded in a 96-well white plate at 5.0×10^3 cells/well. Six hours after seeding the cells, the drugs were added at a 10-µM concentration. Forty-eight hours after for A-549 and 72 h after for the other cell lines, the cells were measured using the CellTiter-Glo® 2.0 reagent. Luminescence measurements were taken 10 min after adding the agent using a microplate reader (BioTek, Gen5 Synergy™ H4, Winooski, VT, USA).

2.4. Data analysis and visualization

Beeswarms and boxplots were created using the beeswarm package and PCA maps were created using the ggplot2 package in the CRAN repository (http://cran.r-project.org/). Heatmaps of the Z-scores were generated using the publicly available software Morpheus (https://software.broadinstitute.org/morpheus/) and hierarchal clustering with the Euclidean distance and an average linkage method. Curve fitting and IC_{50} determinations were performed using the curve fitting analysis tool in Prism 7 (Version 7.0d, GraphPad Software, San Diego, CA, USA). Drug synergism was analyzed using CompuSyn (version 1.0) (http://www.combosyn.com/index.html), which is based on the combination index (CI) theorem of the Chou-Talalay method [23].

2.5. Immunofluorescence

Cells were washed with PBS (−) three times and fixed in 4% paraformaldehyde (Wako) for 15 min at 25 °C. The cells were again washed with PBS (−) three times and treated with 5% BSA (Sigma-Aldrich) and 0.1% Triton X-100 (Sigma-Aldrich) in PBS (−) overnight at 4 °C. The cells were again washed with PBS (−) three times and treated with diluted Anti-Ki-67 antibody (1:250, Abcam, Cambridge, UK) with 5% BSA in PBS (−) for 1–2 h at 37 °C. The staining results were imaged using a BZ-X700 fluorescence microscope (Keyence, Osaka, Japan) using BZ-X analyzer software (Keyence).

2.6. Apoptosis assay measurement in vitro

To evaluate apoptotic activity, a luminescent caspase-3/7 activation assay was performed. The cells were seeded in a white 96-well plate; after 6 h of incubation, selected drugs were added at a concentration of 10 µM. After incubation for 48–72 h, Caspase-Glo® reagent (Caspase-Glo® 3/7 assay; Promega) was added and incubated for 1 h, then the activity of caspase-3/7 was measured using a microplate reader (BioTek, Gen5 Synergy™ H4).

2.7. Western blot analysis

The cells were gently scraped from the culture plates, resuspended in 1000 µL of M-PER buffer, and shaken for 5 min. The samples were then centrifuged at $14,000 \times g$ for 10 min. The supernatants were collected and the protein concentration was calculated using a Qubit 2.0 Fluorometer (Thermo Fisher Scientific, Waltham, MA, USA). Protein extracts (30 µg per lane) were prepared and run on a 4–20% Mini-PROTEAN® TGX™ gel (Bio-Rad, Hercules, CA, USA) or 7.5% Mini-PROTEAN TGX gel (Bio-Rad) then transferred to a 0.45-µm polyvinylidene difluoride (PVDF) membrane. The membranes were blocked for 1 h at 25 °C using Blocking One (Nacalai Tesque, Kyoto, Japan) then incubated overnight at 4 °C with the primary antibodies shown in Table S2. Two secondary antibodies [Anti-Mouse IgG, HRP-Linked Whole Ab Sheep (GE Healthcare, Chicago, IL, USA); and Anti-Rabbit IgG, HRP-Linked Whole Ab Donkey (GE Healthcare)] were used at a dilution of 1:5000 and the membranes were developed using ImmunoStar LD (Wako) and imaged using the FUSION SOLO 7S (Vilber-Lourmat, Marne-la-Vallée, France).

2.8. Crystal violet staining

The cells were seeded in a 6-well plate at 2.0×10^4 cells/well. Six hours after seeding, the cells were treated according to the combinatorial administered dose. Forty-eight hours after culturing, the cells were washed with PBS (−) three times and fixed in 4% paraformaldehyde (Wako) for 15 min at 25 °C. The cells were then washed with PBS and stained with 0.5% crystal violet solution at 25 °C for 30 min. After rinsing with PBS, the plates were photographed using a digital scanner.

2.9. Animal studies

All mouse experiments were approved by the National Cancer Center Research Institute, Institute of Laboratory Animal Research

(Number: T18-009). Five-week-old female BALB/C nude mice were used for animal experiments. A-549 cells (KRAS-mutant) and H-1650 cells (wild-type) were injected into the right flank of the mice with matrigel/PBS (1.0×10^6 cells, 50% final concentration) of each mouse to establish xenograft models. One week after inoculation, each mouse was randomly separated into two groups (n = 6/group) of treatments with vehicle alone (olive oil with 3% DMSO) and with methiazole (total 720 μg/mouse) by intraperitoneal injection. Mice were monitored carefully and the size of their tumors was measured using a Vernier caliper. Tumors were harvested 19 days after inoculation of cancer cells and tumor weight was measured.

2.10. Statistical analysis

The data are presented as mean ± SD. Statistical significance was determined using Student's *t*-test. Differences were considered significant with a p value < 0.05.

3. Results

3.1. Screening of small molecules to identify effective compounds for KRAS-mutant and wild-type cell lines

To perform the screening to discover compounds effective for KRAS-mutant lung cancer cells, we first used three KRAS-mutant (A-549, H-23, and H-1573) and three wild-type (H-1650, H-522, and Calu-3) lung cancer cell lines (Fig. S1A). The screening procedure is summarized in Fig. 1a. Cells seeded in a 96-well white plate were treated with 1271 small molecules at a final concentration of 10 μM for each well. The library was selected because it contained small molecules approved by the FDA, EMA, and other agencies. The data were highly reproducible among independent experiments (Fig. S1B). All the cell lines were screened using the library, cell proliferation was evaluated using an ATP-based assay, and growth inhibition rates were assessed by Z-score analysis (Fig. 1b, Figs. S1C–G). The distributions of the number of compounds according to Z-score analysis obtained from the primary screening are shown in Fig. 1c and Fig. S2A. Most of the compounds (> 80%) from the library that were not effective had a Z-score < 1 and the compounds with a Z-score ≥ 1 were considered for further experimental validation. The compounds with a Z-score ≥ 1 comprised 32% (24/75) oncological compounds and 6% (72/1196) non-oncological compounds and the remainder contained many antitumor compounds, as expected (Fig. 1d). The results of the primary screening were visualized as a heatmap and were represented consistently with a histogram (Fig. 1e).

3.2. Confirmation of the candidate compounds

To investigate the inhibitory effect of compounds from the results of the primary screening, they were analyzed by principal component analysis (PCA). Fig. 2a–c shows the PCA map using Z-score analysis of the inhibitory effect of the compounds. The blue plots in Fig. 2a show all the compounds and the difference between oncological (orange) and nononcological compounds (light blue) is shown in Fig. 2b. The loading profile of PC1 at the x-axis suggests the inhibitory effect of the compounds for both KRAS-mutant and wild-type cells, and PC2 at the y-axis suggests the difference of an inhibitory effect of the compounds between KRAS-mutant and wild-type cells. The average Z-scores of all compounds for KRAS-mutant and wild-type cells are colored according to their distribution range (Fig. 2c). The 50 top-ranked compounds of the average Z-score comprised 11 oncological compounds (15%, 11/75) and 39 nononcological compounds (3%, 39/1196) (Fig. 2d). These results are similar to previous results (Fig. 1d), including commonly used chemotherapeutic agents. Fig. 2e shows the effects of the oncological compounds from the top 50 on cell proliferation. All the top-ranked oncological compounds showed a significant inhibitory effect for both

KRAS-mutant and wild-type cells; the results of the compounds and positive control (cisplatin) used for screening are shown in Fig. S2B.

3.3. KRAS-mutant cells are sensitive to benzimidazole derivatives

Next, we focused on the difference in the compound effects between KRAS-mutant and wild-type cells from the results of the primary screening. An analysis of the Z-scores of the inhibitory effect of the compounds between KRAS-mutant and wild-type cells is shown in volcano plots (Fig. 3a). We identified eight compounds classified by a difference in the Z-score > 0.80 and p-value < 0.05 for subsequent validation assays. Fig. 3b shows the heatmap representing the difference in the average Z-scores of the compounds between KRAS-mutant and wild-type cells. Intriguingly, we found a structural similarity among the selected compounds and most of them were benzimidazole derivatives whose structural formulas are shown in Fig. 3c. The eight selected compounds from the primary screening were tested by cell viability assays using ATP-based experiments; most of them showed a significant difference in their inhibitory effect on cell proliferation between KRAS-mutant and wild-type cells (Fig. 3d, Figs. S3A and B). Taken together, our primary screening and validation assay results indicate that benzimidazole derivatives exhibit a significant difference in their inhibitory effect on cell proliferation between KRAS-mutant and wild-type cells. The more effective chemical compounds, methiazole and fenbendazole, were selected for further validation studies using additional cell lines (Fig. S3C).

3.4. Methiazole and fenbendazole inhibit cell proliferation and induce apoptosis in KRAS-mutant cells

Having demonstrated the effect of benzimidazole derivatives, we sought to perform further analysis for methiazole and fenbendazole. Among the benzimidazole derivatives that show an inhibitory effect on cell proliferation for KRAS-mutant cells, not all of them showed a significant difference between KRAS-mutant and wild-type cells. Given that the compounds with a simpler structure seem to be more effective, we selected methiazole and fenbendazole for subsequent experiments. To validate the effect of methiazole and fenbendazole on KRAS-mutant cells, we performed cell proliferation assays with additional cell lines (KRAS-mutant: A-427, H-1373, H-1734, H-2444, H-2347, A-549, H-23, and H-1573; wild-type: H-1395, H-1435, H-1838, H-2228, H-2286, H-1650, H-522, and Calu-3) (Fig. 4a and Fig. S3C). Both methiazole and fenbendazole showed a significant difference in their inhibitory effect between KRAS-mutant and wild-type cells. To further evaluate the function of benzimidazole derivatives, we performed immuno-fluorescence for Ki-67 of KRAS-mutant cell lines (A-549 and H-23) and wild-type cell lines (H-1650 and H-2228) after treatment with methiazole and fenbendazole. Ki-67-positive cells were reduced significantly in KRAS-mutant cells compared to wild-type cells; furthermore, morphological changes were observed upon treatment with methiazole and fenbendazole, while no changes were observed upon treatment with DMSO (Fig. 4b and Fig. S4A). We next sought to determine the cellular effects (cytotoxicity or cytostasis) of methiazole and fenbendazole. Apoptosis after treatment with methiazole and fenbendazole was analyzed based on nuclear DNA fragmentation (Fig. S4). These experiments in other cell lines as well as treatment with fenbendazole also reduced Ki-67-positive cells (Figs. S4A and B). To confirm apoptotic cell death after the treatments, we performed a caspase 3/7 assay and nuclear DNA fragmentation counting. KRAS-mutant cells showed significantly higher caspase 3/7 activity and greater numbers of apoptotic cells than wild-type cells (Figs. S4C–E). These results suggest that benzimidazole derivatives inhibit cell proliferation and induce apoptosis via caspase 3/7 activity. The above results indicate that methiazole and fenbendazole have more inhibitory effects on KRAS-mutant cells than on wild-type cells and cause cytotoxicity via apoptosis. Regarding methiazole and fenbendazole, the IC_{50} was determined
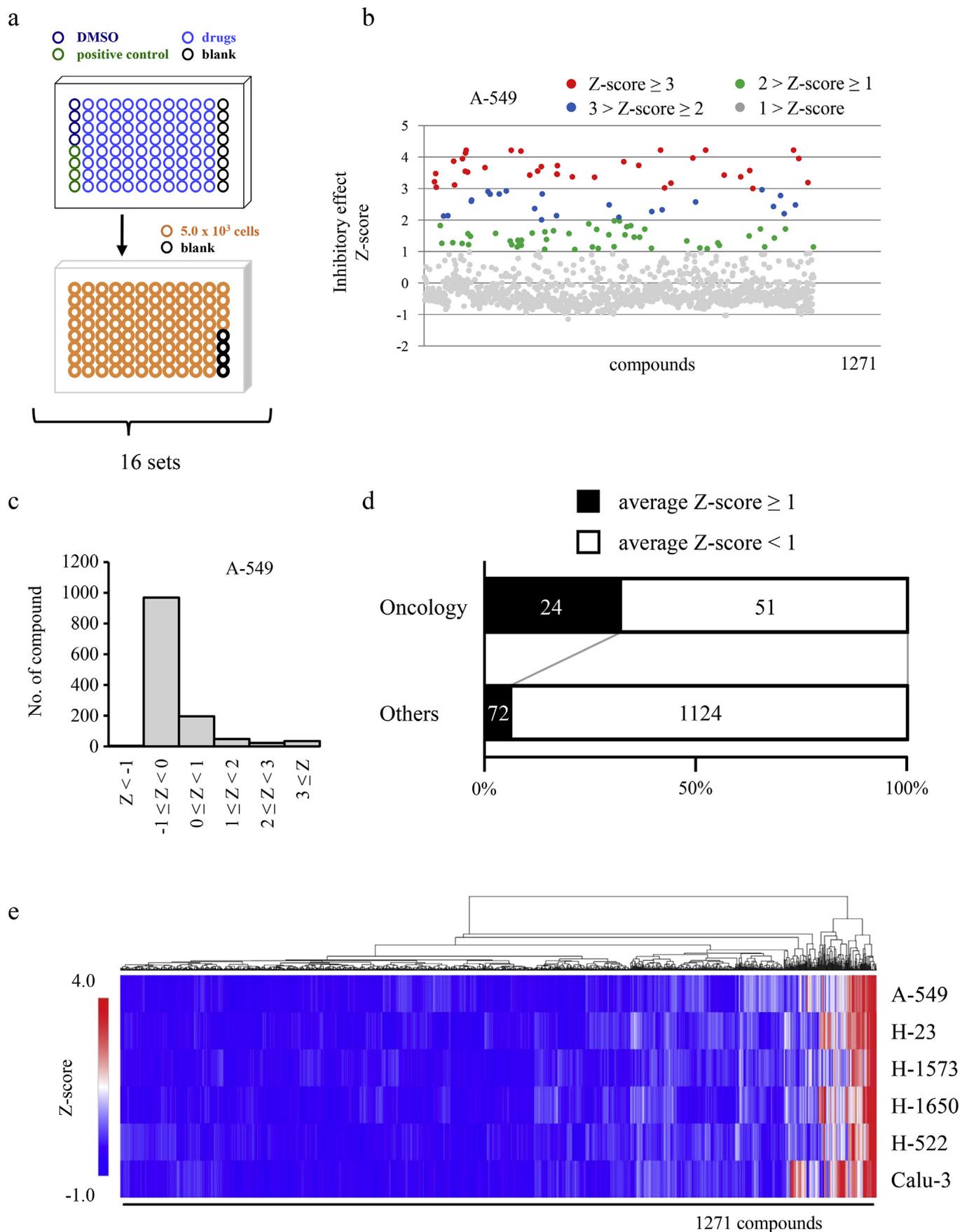
Fig. 1. Screening to identify compounds from a small-molecule library that inhibits the proliferation of both KRAS-mutant and wild-type cells. a. Schematic overview of the protocol used for screening. **b.** Graph showing the Z-scores of the inhibitory effect of the compounds from the primary screen for A-549. **c.** Histogram of the Z-scores of the compounds for A-549. **d.** Ratio of the compounds with an average Z-score ≥ 1 in oncological compounds and non-oncological compounds. **e.** Heatmap showing the effect of compounds in KRAS-mutant and wild-type cell lines.
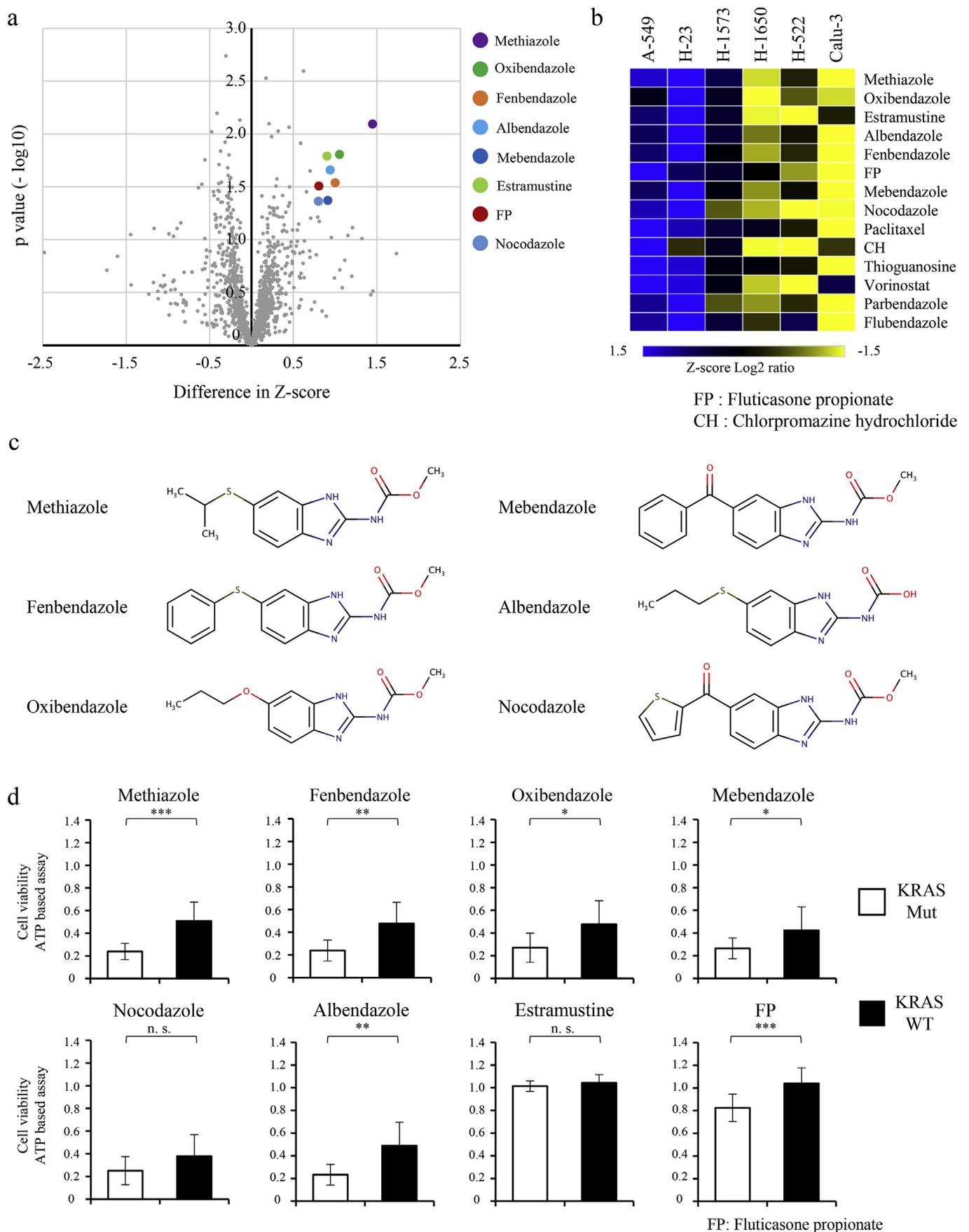
Fig. 2. Highly effective compounds from primary screening. a. PCA analysis of all screened compounds. **b**. PCA analysis of oncological compounds and non-oncological compounds. **c**. PCA analysis of effective compounds for KRAS-mutant and wild-type cells. **d**. Fifty top ranked compounds that inhibit cell proliferation. **e**. Inhibitory effect of the selected compounds in oncological fields relative to control.

Fig. 3. Benzimidazole derivatives are more effective in KRAS-mutant cells. a. Difference in the effect of compounds between KRAS-mutant and wild-type cells. b. Clustering analysis of the selected compounds. c. Structure of the benzimidazole derivatives. d. Quantitative effect of the selected compounds on cell proliferation. The values are mean ± SD (n = 4). *, p < 0.05; **, p < 0.01; ***, p < 0.001; and n.s., not significant.
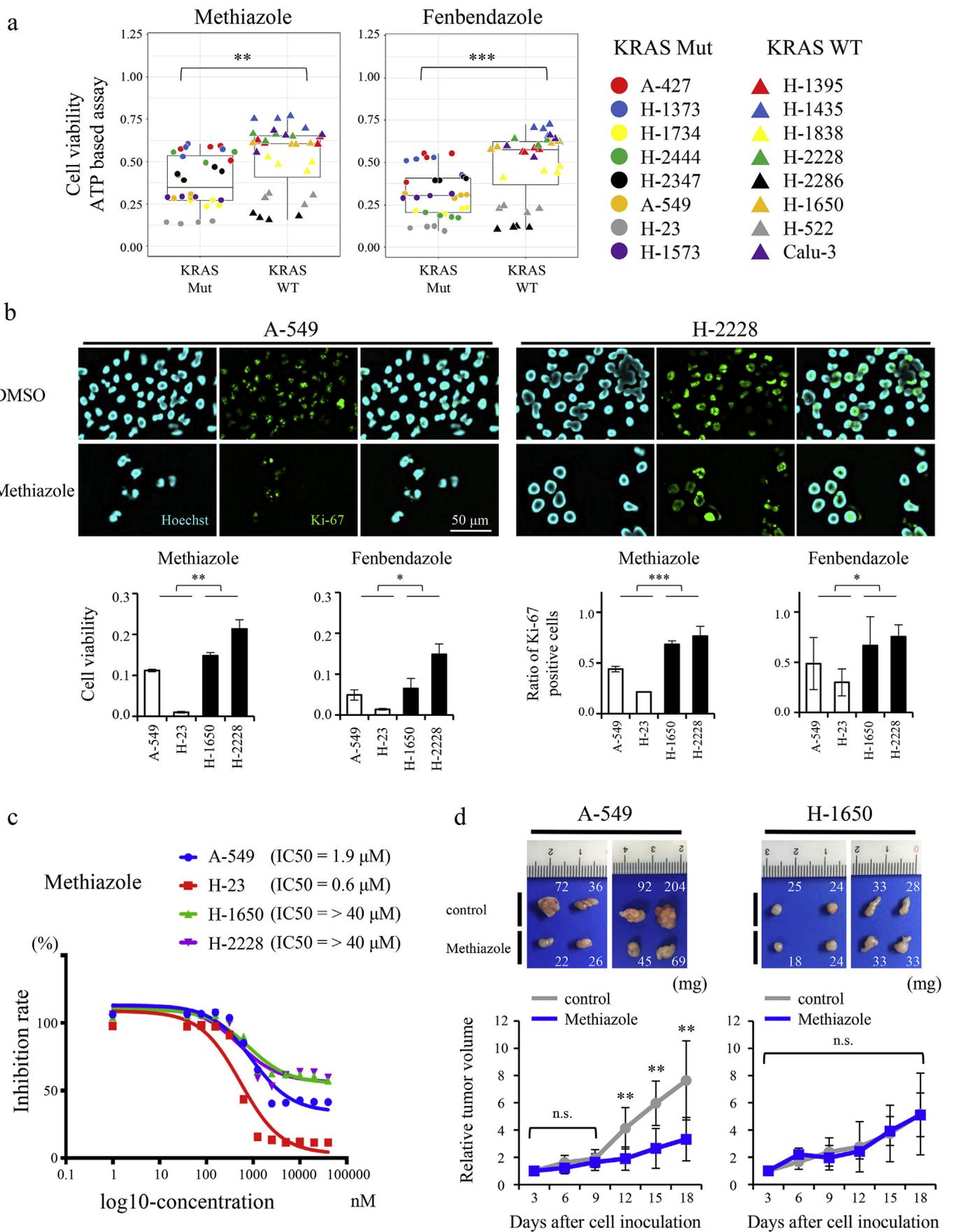
(caption on next page)

Fig. 4. Methiazole and fenbendazole are more effective in KRAS-mutant cells. a. Quantification of the proliferation rate following treatment with methiazole and fenbendazole in KRAS-mutant and wild-type cells. The values are mean ± SD (n = 4). **, p < 0.01; ***, p < 0.001. **b**. Effects of methiazole and fenbendazole on the proliferation of A-549 and H-2228 cells as determined by Ki-67 analyses. The values are mean ± SD (n = 3). *, p < 0.05; **, p < 0.01; ***, p < 0.001. **c**. The cells were treated with increasing doses of methiazole. Cell viability was determined using an ATP-based assay. The values are mean ± SD (n = 4). **d**. Quantitative analysis of tumor progression starting from the first instance at which a solid tumor mass was identified. Data shown are normalized to pretreatment tumor mass on day three from cell inoculation. Representative images of dissected tumors are shown in upper panels. The values are mean ± SD (n = 6). **, p < 0.01; and n.s., not significant.

by inhibition curves drawn based on the results of the cell viability assay. We found that KRAS-mutant cells were more sensitive to methiazole (A-549: 1.9 μM; H-23: 0.6 μM) and fenbendazole (A-549: 1.5 μM; H-23: 0.4 μM), and the IC_{50} values were much lower than those of wild-type cells (methiazole = H-1650: > 40 μM, H-2228: > 40 μM; fenbendazole = H-1650: 6.2 μM, H-2228: 7.8 μM) (Fig. 4c and Fig. S5). We also evaluated the in vivo therapeutic effects of the benzimidazole derivatives in a subcutaneous xenograft model. We treated A-549 (KRAS-mutant) and H-1650 (wild-type)-xenografted mice with methiazole according to the protocol shown in Fig. S6A. As expected, the tumor size in A-549-xenografted mice was significantly decreased (Fig. 4d lower panels) while that in H-1650-xenografted mice was unchanged. Although the tumor weight tended to decrease in A-549-xenografted mice, the change was not statistically significant (Fig. 4d upper panels and S6B).

3.5. Structural specificity of the benzimidazole derivatives

To further understand the structural relationship between the benzimidazole derivatives and KRAS-mutant and wild-type cells, the effects of other benzimidazole derivatives were also examined. Given that methiazole and fenbendazole have relatively simple structures, these compounds were considered. Benzimidazole and carbendazim, two benzimidazole derivatives, are also structurally simple, and, were used for the analysis (Fig. S7A). To investigate the biological characteristics of benzimidazole and carbendazim, the same experiments as those for methiazole and fenbendazole were performed. From the results of an ATP-based cell proliferation assay, benzimidazole was found not to affect the cell proliferation in both KRAS-mutant and wild-type cells, while carbendazim inhibited cell proliferation but showed no difference between KRAS-mutant and wild-type cells (Fig. 5a). No effect was observed for Ki-67 immunofluorescence and apoptotic cells treated with benzimidazole. Similar to the ATP-based cell proliferation assay, carbendazim inhibited cell proliferation and induced cell apoptosis, but there was no significant difference between KRAS-mutant and wild-type cells (Fig. 5b and Fig. S7B). Cell viability and caspase 3/7 activity were also consistent with the results described above (Figs. S7C and D). Furthermore, cell proliferation assays including compounds with an imidazole structure revealed that not all compounds demonstrated cytotoxicity and only certain compounds among the benzimidazole derivatives showed inhibitory effects on KRAS-mutant cells (Fig. 5c and Fig. S7E). Importantly, methiazole exhibited almost no cytotoxic effects on normal epithelial cells compared with cisplatin (Fig. S7F), while fenbendazole possessed slightly higher cytotoxicity. According to these results, it was suggested that the structural components contained in methiazole and fenbendazole may contribute to RAS selectivity because no significance was observed in the analysis of benzimidazole and carbendazim between KRAS-mutant and wild-type cells.

3.6. Methiazole and fenbendazole affect RAS signaling and exhibit synergy when combined with a MEK inhibitor

To explore the differences in the mechanisms of these compounds between KRAS-mutant and wild-type lung cancer cells, we performed western blot analysis after treatment with methiazole, fenbendazole, benzimidazole, and carbendazim. We examined the status of the PI3K/AKT and RAF/MEK/ERK pathways to assess the effect of these

compounds (Fig. 6a). Treatment of KRAS-mutant cells (H-23) with methiazole and fenbendazole simultaneously suppressed the PI3K/AKT pathway (confirmed by low levels of phosphorylated AKT), RAF/MEK/ERK pathway (verified by low levels of phosphorylated ERK), and Stat1 levels. SAPK, NFκB, and PI3Ks exhibited no specific differences upon treatment with the drugs (Fig. S8A). Benzimidazole and carbendazim showed little or no reduction effect in both KRAS-mutant and wild-type cells. These results indicate that benzimidazole derivatives, especially methiazole and fenbendazole, inhibit the PI3K/AKT and RAF/MEK/ERK pathways compared with the normal control (Fig. 6b).

Given that methiazole and fenbendazole could partly suppress KRAS downstream signaling, the data prompted us to test the combinatorial effects of the benzimidazole derivatives with RAS signaling-related tyrosine kinase inhibitors such as vemurafenib, dabrafenib, and trametinib. Upon various combinations of these drugs, most exerted synergistic effects at high concentrations (Fig. S8B); however, the combination of methiazole with trametinib, a MEK inhibitor, showed a maximum synergistic effect even at a low concentration based on the calculations using the median-effect principle and combination index-isobologram theorem (Fig. 6c and Fig. S9). Thus, the combinatorial treatment of methiazole and fenbendazole with tyrosine kinase inhibitors, especially trametinib, may offer a novel therapeutic strategy.

4. Discussion

Despite years of developmental work on KRAS-mutant lung cancer, the effective targeting of the molecular driver of KRAS in lung cancer cells remains unsuccessful [24]. Extensive efforts have been directed toward the identification of new strategies, such as synthetic lethal target interactions with oncogenic KRAS-expressing cells [25,26]. The identification of small molecules that affect KRAS or KRAS-related signaling pathways would be a step in this direction. Through drug library screening, we have demonstrated that benzimidazole derivatives serve as selective cytotoxic agents for KRAS-mutant lung cancer cells. Benzimidazole derivatives induce apoptotic cell death and inhibit KRAS-mutant lung cancer cell proliferation. We identified that methiazole and fenbendazole significantly inhibit the expression of the RAS-related signaling pathway in KRAS-mutant lung cancer cells. Consistent with the in vitro experiments, treatment with methiazole showed significant inhibitory effects in vivo. The combinatorial treatment of tyrosine kinase inhibitors, especially trametinib with methiazole, showed synergistic effects in KRAS-mutant lung cancer cells. Presently, there is no effective direct therapy for KRAS-mutant lung cancer cells though multiple strategies have been employed to identify such candidate inhibitors using high-throughput screening, fragment-based screening, or in silico screening [27]. Here, we showed the effectiveness of a phenotypic approach using a drug library and identified an effective combination strategy in KRAS-mutant lung cancer cells.

As previously reported, benzimidazole derivatives are commonly used as anthelmintic therapeutics against roundworms and tapeworms in animals and humans [28,29]. Recently, these compounds have been identified as potent anticancer agents and their mechanism of antitumor activity may be through the binding of tubulin [30,31], inhibition of poly (ADP-ribose) polymerase-1 (PARP-1) [32], topoisomerase I [33], and tyrosine kinases [34]. Several studies have shown that benzimidazole derivatives may serve as novel agents for anticancer therapy [35]. Most of the clinically approved kinase inhibitors include bicyclic
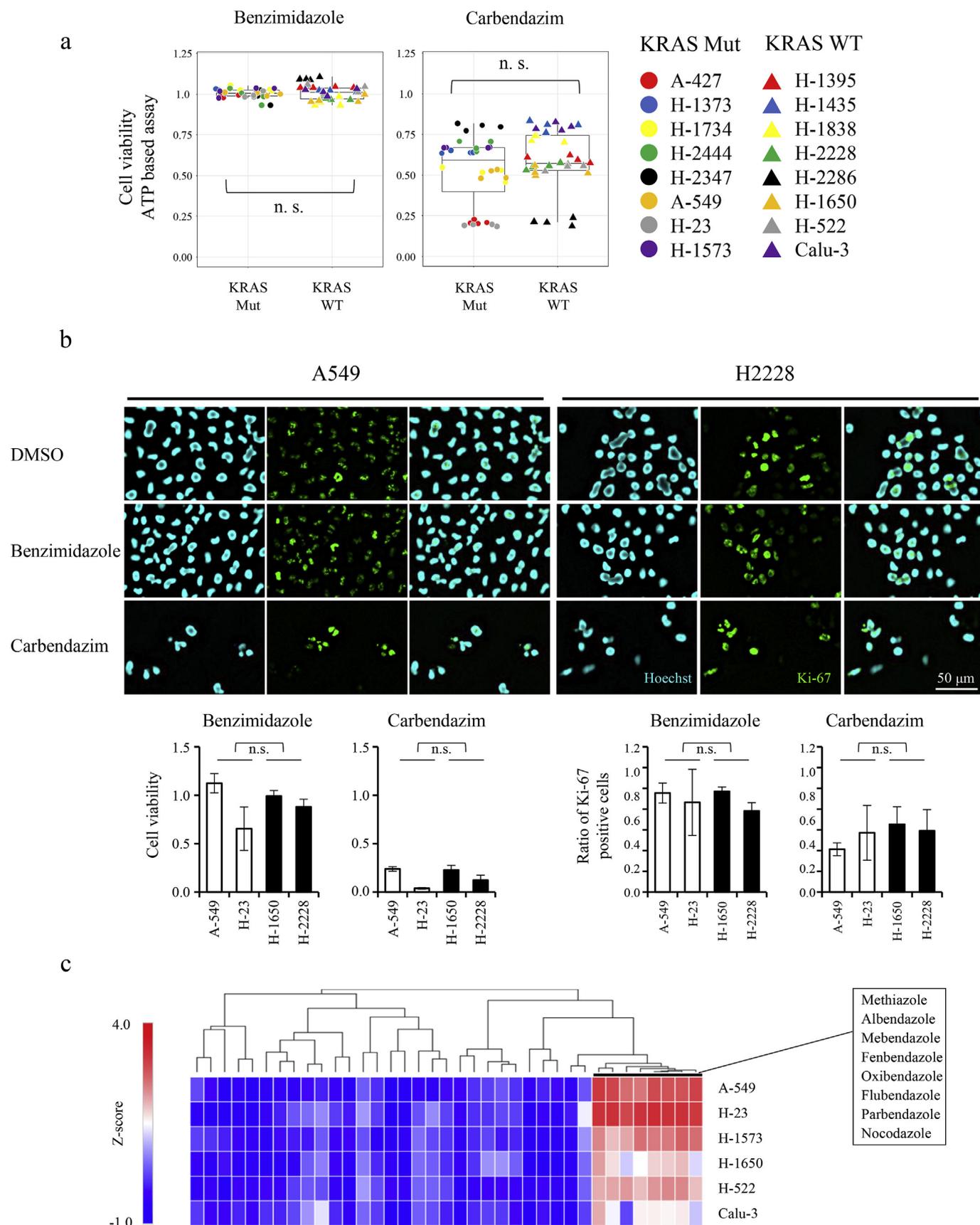
Fig. 5. Analysis of the structural differences in the benzimidazole derivatives. a. Quantification of the proliferation rate following treatment with benzimidazole and carbendazim in KRAS-mutant and wild-type cells. **b**. Effects of benzimidazole and carbendazim on the proliferation of A-549 and H-2228 cells as determined by Ki-67 analyses. The values are mean ± SD (n = 3). n.s., not significant. **c**. Only certain compounds of benzimidazole derivatives showed inhibitory effects on both KRAS-mutant and wild-type cells.
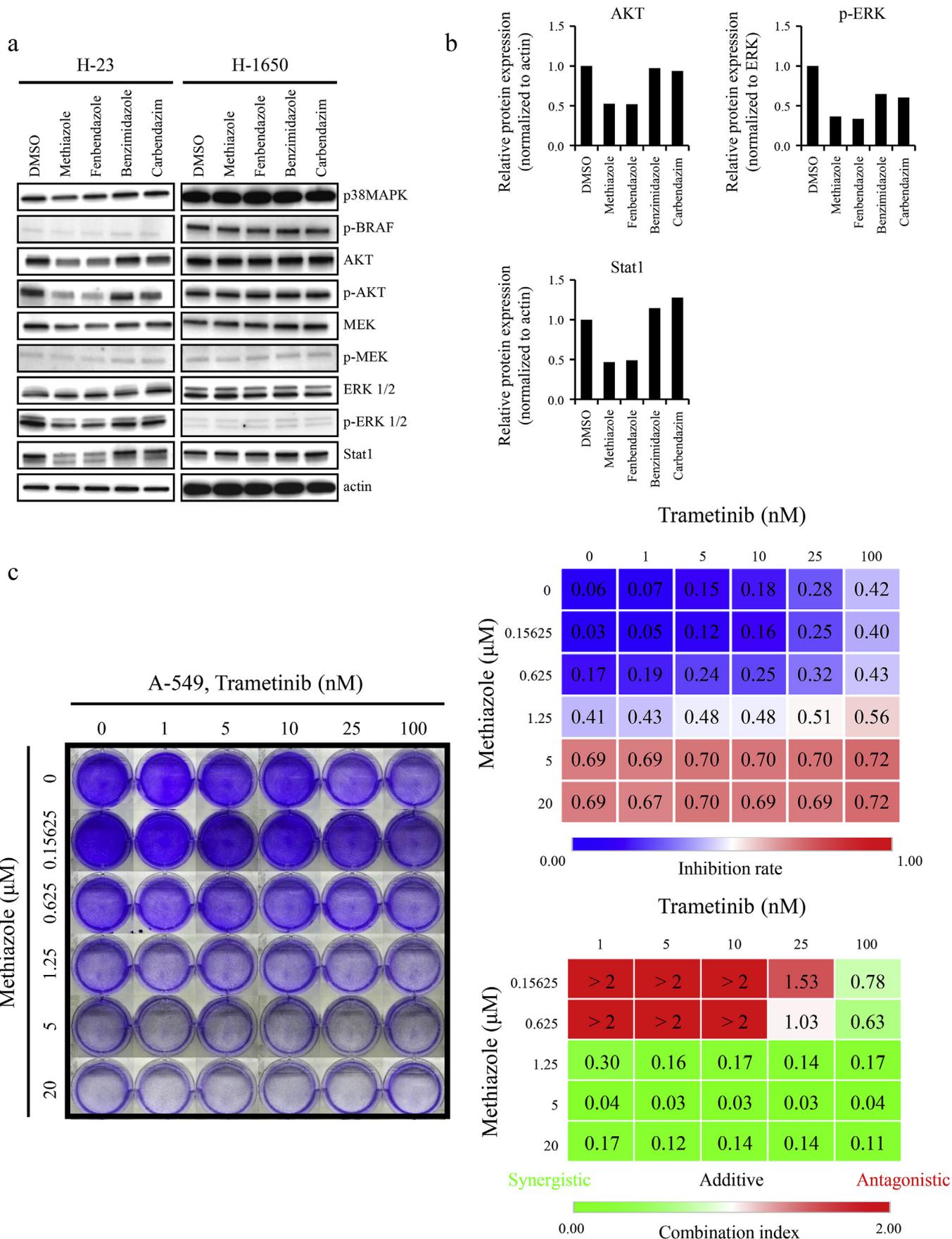
Fig. 6. Effects of methiazole and fenbendazole on RAS-related signaling. a. Western blot analyses of RAS-related signaling in H-23 and H-1650 cell lines treated with benzimidazole derivatives. **b**. Quantification of the blots of p-AKT, p-ERK, and Stat1. **c**. Image of the combinatorial experiment of methiazole and trametinib in A-549 cells. Data of the combinatorial experiment and combination index scores for A-549 cells treated with methiazole and trametinib at the indicated concentrations.

nitrogen heterocycles, but the benzimidazole scaffold interacts with kinases using multiple binding modes [36]. Regarding the recently developed molecular target therapeutic approach, some benzimidazole derivatives have been synthesized as kinase inhibitors, protein kinase CK2 (casein kinase 2) inhibitors [37], CDK9 (cyclin-dependent kinase 9) inhibitors [38], and multi target kinase inhibitors [34,39]. Given that the benzimidazole derivatives identified in the primary screening exhibited antitumor effects and there are relatively few reports on methiazole and fenbendazole, we tried to assess their functional mechanisms. It is worth noting that methiazole and fenbendazole possess significant inhibitory effects on KRAS-mutant lung cancer cells. In the era of molecular target-based strategies in NSCLC, attempts to inhibit downstream effector pathways have shown only limited success [40]. However, the results of treatment with methiazole and fenbendazole in KRAS-mutant lung cancer cells clearly revealed the suppression of the PI3K/AKT and RAF/MEK/ERK pathways, both RAS-dependent pathways, indicating the underlying mechanism of the compound effects. The analysis of the structurally simpler compounds of benzimidazole derivatives, benzimidazole and carbendazim, as well as other compounds having an imidazole structure, showed that, among the benzimidazole derivatives, there is a structural specificity in the inhibitory effect on cell proliferation that differs between the presence and absence of KRAS mutation.

Combinatorial experiments with methiazole, fenbendazole, and tyrosine kinase inhibitors revealed synergistic effects for KRAS-mutant lung cancer cells (Fig. 6c and Fig. S8B). Although most of the strategies targeting mutant KRAS had a low specificity or less therapeutic efficacy, treatment modalities based on synthetic lethal interaction have been explored [25,26,41]. Given that methiazole and fenbendazole suppress the protein expression of AKT and ERK in the RAS-related signaling pathways of the RAF/MEK/ERK and PI3K/AKT pathways, we performed combinational experiments using several tyrosine kinase inhibitors. Synergistic cytotoxic effects on KRAS-mutant lung cancer cells were observed upon combination and methiazole or fenbendazole with trametinib, a MEK inhibitor, showed a highly synergistic effect at low concentration. As a substitute for a direct target to attack RAS proteins themselves, the MAPK pathway components RAF, MEK, and ERK and PI3K pathway components were expected to act as alternative targets. However, these pathways are much more complicated and various studies have attempted to confirm the interaction of these pathways [42–44]. Our data shed light on the ability of the combinatorial treatment of benzimidazole derivatives and a MEK inhibitor. Another study reported that a synthetic lethal approach targeting MEK and FGFR1 is effective for KRAS driven cancer cells [45]; however, further synergistic or synthetic lethal analysis for KRAS-related oncogenesis is warranted.

Author contributions

I.S., Y.Y., I.K., M.K., and Y.A. designed, performed and analyzed experiments. Y.T. and K.T. designed experiments and helped with critical advice and discussion. The manuscript was finalized by T.O. with the assistance of all of the authors. All authors read and approved the final manuscript.

Competing interests

The authors declare that they have no competing interests.

Declarations of interest

None.

Acknowledgements

Appendix A. Supplementary data

Supplementary data to this article can be found online at https://doi.org/10.1016/j.canlet.2019.03.002.

References

[1] L.A. Torre, F. Bray, R.L. Siegel, J. Ferlay, J. Lortet-Tieulent, A. Jemal, Global cancer statistics, 2012, CA A Cancer J. Clin. 65 (2015) 87–108.

[2] J.H. Schiller, D. Harrington, C.P. Belani, C. Langer, A. Sandler, J. Krook, J. Zhu, D.H. Johnson, Comparison of four chemotherapy regimens for advanced non-small-cell lung cancer, N. Engl. J. Med. 346 (2002) 92–98.

[3] L.A. Torre, R.L. Siegel, A. Jemal, Lung cancer statistics, Adv. Exp. Med. Biol. 893 (2016) 1–19.

[4] G.M. Stella, M. Luisetti, S. Inghilleri, F. Cemmi, R. Scabini, M. Zorzetto, E. Pozzi, Targeting EGFR in non-small-cell lung cancer: lessons, experiences, strategies, Respir. Med. 106 (2012) 173–183.

[5] J.G. Paez, P.A. Janne, J.C. Lee, S. Tracy, H. Greulich, S. Gabriel, P. Herman, F.J. Kaye, N. Lindeman, T.J. Boggon, K. Naoki, H. Sasaki, Y. Fujii, M.J. Eck, W.R. Sellers, B.E. Johnson, M. Meyerson, EGFR mutations in lung cancer: correlation with clinical response to gefitinib therapy, Science (New York, N.Y.) 304 (2004) 1497–1500.

[6] M. Soda, Y.L. Choi, M. Enomoto, S. Takada, Y. Yamashita, S. Ishikawa, S. Fujiwara, H. Watanabe, K. Kurashina, H. Hatanaka, M. Bando, S. Ohno, Y. Ishikawa, H. Aburatani, T. Niki, Y. Sohara, Y. Sugiyama, H. Mano, Identification of the transforming EML4-ALK fusion gene in non-small-cell lung cancer, Nature 448 (2007) 561–566.

[7] T.J. Lynch, D.W. Bell, R. Sordella, S. Gurubhagavatula, R.A. Okimoto, B.W. Brannigan, P.L. Harris, S.M. Haserlat, J.G. Supko, F.G. Haluska, D.N. Louis, D.C. Christiani, J. Settleman, D.A. Haber, Activating mutations in the epidermal growth factor receptor underlying responsiveness of non-small-cell lung cancer to gefitinib, N. Engl. J. Med. 350 (2004) 2129–2139.

[8] B.J. Solomon, T. Mok, D.W. Kim, Y.L. Wu, K. Nakagawa, T. Mekhail, E. Felip, F. Cappuzzo, J. Paolini, T. Usari, S. Iyer, A. Reisman, K.D. Wilner, J. Tursi, F. Blackhall, First-line crizotinib versus chemotherapy in ALK-positive lung cancer, N. Engl. J. Med. 371 (2014) 2167–2177.

[9] C.G.A.R. Network, Comprehensive molecular profiling of lung adenocarcinoma, Nature 511 (2014) 543–550.

[10] S. Dogan, R. Shen, D.C. Ang, M.L. Johnson, S.P. D'Angelo, P.K. Paik, E.B. Brzostowski, G.J. Riely, M.G. Kris, M.F. Zakowski, M. Ladanyi, Molecular epidemiology of EGFR and KRAS mutations in 3,026 lung adenocarcinomas: higher susceptibility of women to smoking-related KRAS-mutant cancers, Clin. Cancer Res.: Off. J. Am. Assoc. Canc. Res. 18 (2012) 6169–6177.

[11] M. Imielinski, A.H. Berger, P.S. Hammerman, B. Hernandez, T.J. Pugh, E. Hodis, J. Cho, J. Suh, M. Capelletti, A. Sivachenko, C. Sougnez, D. Auclair, M.S. Lawrence, P. Stojanov, K. Cibulskis, K. Choi, L. de Waal, T. Sharifnia, A. Brooks, H. Greulich, S. Banerji, T. Zander, D. Seidel, F. Leenders, S. Ansen, C. Ludwig, W. Engel-Riedel, E. Stoelben, J. Wolf, C. Goparju, K. Thompson, W. Winckler, D. Kwiatkowski, B.E. Johnson, P.A. Janne, V.A. Miller, W. Pao, W.D. Travis, H.I. Pass, S.B. Gabriel, E.S. Lander, R.K. Thomas, L.A. Garraway, G. Getz, M. Meyerson, Mapping the hallmarks of lung adenocarcinoma with massively parallel sequencing, Cell 150 (2012) 1107–1120.

[12] J. Downward, Targeting RAS signalling pathways in cancer therapy, Nat. Rev. Canc. 3 (2003) 11–22.

[13] A G Stephen, D. Esposito, R.K. Bagni, F. McCormick, Dragging ras back in the ring, Cancer Cell 25 (2014) 272–281.

[14] J. Luo, M.J. Emanuele, D. Li, C.J. Creighton, M.R. Schlabach, T.F. Westbrook, K.K. Wong, S.J. Elledge, A genome-wide RNAi screen identifies multiple synthetic lethal interactions with the Ras oncogene, Cell 137 (2009) 835–848.

[15] M. Malumbres, M. Barbacid, RAS oncogenes: the first 30 years, Nat. Rev. Canc. 3 (2003) 459–465.

[16] D.A. Tuveson, A.T. Shaw, N.A. Willis, D.P. Silver, E.L. Jackson, S. Chang, K.L. Mercer, R. Grochow, H. Hock, D. Crowley, S.R. Hingorani, T. Zaks, C. King, M.A. Jacobetz, L. Wang, R.T. Bronson, S.H. Orkin, R.A. DePinho, T. Jacks, Endogenous oncogenic K-ras(G12D) stimulates proliferation and widespread neoplastic and developmental defects, Cancer Cell 5 (2004) 375–387.

[17] N.T. Ihle, L.A. Byers, E.S. Kim, P. Saintigny, J.J. Lee, G.R. Blumenschein, A. Tsao, S. Liu, J.E. Larsen, J. Wang, L. Diao, K.R. Coombes, L. Chen, S. Zhang, M.F. Abdelmelek, X. Tang, V. Papadimitrakopoulou, J.D. Minna, S.M. Lippman, W.K. Hong, R.S. Herbst, I.I. Wistuba, J.V. Heymach, G. Powis, Effect of KRAS oncogene substitutions on protein behavior: implications for signaling and clinical outcome, J. Natl. Cancer Inst. 104 (2012) 228–239.

[18] P.J. Roberts, C.J. Der, Targeting the Raf-MEK-ERK mitogen-activated protein kinase cascade for the treatment of cancer, Oncogene 26 (2007) 3291–3310.

[19] P. Liu, H. Cheng, T.M. Roberts, J.J. Zhao, Targeting the phosphoinositide 3-kinase pathway in cancer, Nat. Rev. Drug Discov. 8 (2009) 627–644.

[20] J. Zhang, P.L. Yang, N.S. Gray, Targeting cancer with small molecule kinase

inhibitors, Nat. Rev. Canc. 9 (2009) 28–39.

[21] D.C. Swinney, Phenotypic vs. target-based drug discovery for first-in-class medicines, Clin. Pharmacol. Therapeut. 93 (2013) 299–301.

[22] L.H. Jones, M.E. Bunnage, Applications of chemogenomic library screening in drug discovery, Nat. Rev. Drug Discov. 16 (2017) 285–296.

[23] T.C. Chou, Drug combination studies and their synergy quantification using the Chou-Talalay method, Cancer Res. 70 (2010) 440–446.

[24] A.D. Cox, S.W. Fesik, A.C. Kimmelman, J. Luo, C.J. Der, Drugging the undruggable RAS: mission possible? Nat. Rev. Drug Discov. 13 (2014) 828–851.

[25] C. Scholl, S. Frohling, I.F. Dunn, A.C. Schinzel, D.A. Barbie, S.Y. Kim, S.J. Silver, P. Tamayo, R.C. Wadlow, S. Ramaswamy, K. Dohner, L. Bullinger, P. Sandy, J.S. Boehm, D.E. Root, T. Jacks, W.C. Hahn, D.G. Gilliland, Synthetic lethal interaction between oncogenic KRAS dependency and STK33 suppression in human cancer cells, Cell 137 (2009) 821–834.

[26] M. Puyol, A. Martin, P. Dubus, F. Mulero, P. Pizcueta, G. Khan, C. Guerra, D. Santamaria, M. Barbacid, A synthetic lethal interaction between K-Ras oncogenes and Cdk4 unveils a therapeutic strategy for non-small cell lung carcinoma, Cancer Cell 18 (2010) 63–73.

[27] M. Holderfield, Efforts to develop KRAS inhibitors, Cold Spring Harbor Perspect. Med. 8 (2018).

[28] Y. Bansal, O. Silakari, The therapeutic journey of benzimidazoles: a review, Bioorg. Med. Chem. 20 (2012) 6208–6236.

[29] W.C. Campbell, Benzimidazoles: veterinary uses, Parasitol. today (Personal ed.) 6 (1990) 130–133.

[30] W. Wang, D. Kong, H. Cheng, L. Tan, Z. Zhang, X. Zhuang, H. Long, Y. Zhou, Y. Xu, X. Yang, K. Ding, New benzimidazole-2-urea derivates as tubulin inhibitors, Bioorg. Med. Chem. Lett 24 (2014) 4250–4253.

[31] J. Sasaki, R. Ramesh, S. Chada, Y. Gomyo, J.A. Roth, T. Mukhopadhyay, The anthelmintic drug mebendazole induces mitotic arrest and apoptosis by depolymerizing tubulin in non-small cell lung cancer cells, Mol. Canc. Therapeut. 1 (2002) 1201–1209.

[32] A.W. White, N.J. Curtin, B.W. Eastman, B.T. Golding, Z. Hostomsky, S. Kyle, J. Li, K.A. Maegley, D.J. Skalitzky, S.E. Webber, X.H. Yu, R.J. Griffin, Potentiation of cytotoxic drug activity in human tumour cell lines, by amine-substituted 2-arylbenzimidazole-4-carboxamide PARP-1 inhibitors, Bioorg. Med. Chem. Lett 14 (2004) 2433–2437.

[33] J.S. Kim, B. Gatto, C. Yu, A. Liu, L.F. Liu, E.J. LaVoie, Substituted 2,5'-Bi-1H-benzimidazoles: topoisomerase I inhibition and cytotoxicity, J. Med. Chem. 39 (1996) 992–998.

[34] Y. Li, C. Tan, C. Gao, C. Zhang, X. Luan, X. Chen, H. Liu, Y. Chen, Y. Jiang, Discovery of benzimidazole derivatives as novel multi-target EGFR, VEGFR-2 and PDGFR kinase inhibitors, Bioorg. Med. Chem. 19 (2011) 4529–4535.

[35] S. Yadav, B. Narasimhan, H. Kaur, Perspectives of benzimidazole derivatives as anticancer agents in the new era, Anti Cancer Agents Med. Chem. 16 (2016) 1403–1425.

[36] L. Garuti, M. Roberti, G. Bottegoni, Benzimidazole derivatives as kinase inhibitors, Curr. Med. Chem. 21 (2014) 2284–2298.

[37] K. Kubinski, M. Maslyk, A. Orzeszko, Benzimidazole inhibitors of protein kinase CK2 potently inhibit the activity of atypical protein kinase Rio1, Mol. Cell. Biochem. 426 (2017) 195–203.

[38] Y.A. Sonawane, M.A. Taylor, J.V. Napoleon, S. Rana, J.I. Contreras, A. Natarajan, Cyclin dependent kinase 9 inhibitors for cancer therapy, J. Med. Chem. 59 (2016) 8667–8684.

[39] B. Chu, F. Liu, L. Li, C. Ding, K. Chen, Q. Sun, Z. Shen, Y. Tan, C. Tan, Y. Jiang, A benzimidazole derivative exhibiting antitumor activity blocks EGFR and HER2 activity and upregulates DR5 in breast cancer cells, Cell Death Dis. 6 (2015) e1686.

[40] F. McCormick, KRAS as a therapeutic target, Clin. Cancer Res.: Off. J. Am. Assoc. Canc. Res. 21 (2015) 1797–1801.

[41] D.A. Barbie, P. Tamayo, J.S. Boehm, S.Y. Kim, S.E. Moody, I.F. Dunn, A.C. Schinzel, P. Sandy, E. Meylan, C. Scholl, S. Frohling, E.M. Chan, M.L. Sos, K. Michel, C. Mermel, S.J. Silver, B.A. Weir, J.H. Reiling, Q. Sheng, P.B. Gupta, R.C. Wadlow, H. Le, S. Hoersch, B.S. Wittner, S. Ramaswamy, D.M. Livingston, D.M. Sabatini, M. Meyerson, R.K. Thomas, E.S. Lander, J.P. Mesirov, D.E. Root, D.G. Gilliland, T. Jacks, W.C. Hahn, Systematic RNA interference reveals that oncogenic KRAS-driven cancers require TBK1, Nature 462 (2009) 108–112.

[42] P. Lito, N. Rosen, D.B. Solit, Tumor adaptation and resistance to RAF inhibitors, Nat. Med. 19 (2013) 1401–1409.

[43] P. Lito, A. Saborowski, J. Yue, M. Solomon, E. Joseph, S. Gadal, M. Saborowski, E. Kastenhuber, C. Fellmann, K. Ohara, K. Morikami, T. Miura, C. Lukacs, N. Ishii, S. Lowe, N. Rosen, Disruption of CRAF-mediated MEK activation is required for effective MEK inhibition in KRAS mutant tumors, Cancer Cell 25 (2014) 697–710.

[44] E. Castellano, C. Sheridan, M.Z. Thin, E. Nye, B. Spencer-Dene, M.E. Diefenbacher, C. Moore, M.S. Kumar, M.M. Murillo, E. Gronroos, F. Lassailly, G. Stamp, J. Downward, Requirement for interaction of PI3-kinase p110alpha with RAS in lung tumor maintenance, Cancer Cell 24 (2013) 617–630.

[45] E. Manchado, S. Weissmueller, J.P.t. Morris, C.C. Chen, R. Wullenkord, A. Lujambio, E. de Stanchina, J.T. Poirier, J.F. Gainor, R.B. Corcoran, J.A. Engelman, C.M. Rudin, N. Rosen, S.W. Lowe, A combinatorial strategy for treating KRAS-mutant lung cancer, Nature 534 (2016) 647–651.